Received: 20-02-2024; Accepted: 06-08-2024

https://doi.org/10.56024/ispm.74.3ampersand4.2024/61-75

Comparative microstructural analysis of *Camellia sinensis* leaves across different nodes

Karishma Khan | Himanshu Dawda | Usha Mukundan

Department of Botany, Plant Biotechnology Laboratory, Ramniranjan Jhunjhunwala College (Empowered autonomous), Ghatkopar (West), Mumbai, 400086, India

Author for correspondence: Karishma Khan Department of Botany, Plant Biotechnology Laboratory, Ramniranjan Jhunjhunwala College (Empowered autonomous), Ghatkopar (West), Mumbai, 400086, India
E-mail:
karishmarajbhar@rjcollege.edu.in

Abstract

Tea, esteemed for its therapeutic properties, enjoys widespread consumption worldwide. Derived from the dried leaves of *Camellia sinensis*, it boasts a rich composition of polyphenols, including flavanols, gallic acid, and catechins, with epigallocatechin-3-gallate (EGCG) standing out as the most prevalent catechin. Microscopic analysis reveals that while young leaves exhibit fewer microstructures, older leaves showcase well-developed and diverse formations.

Keywords: Anatomy, *Camellia sinensis*, Druses, Leaf Node, Microstructures, Tea

Introduction

The tea plant, *Camellia sinensis* from Theaceae family, is a versatile species from which black, oolong, and green teas are derived. While it can reach heights of up to 30 feet, it is typically pruned to a more manageable height of around two meters to facilitate harvesting. The leaves of the tea plant are characterised by their dark green colour, alternate stem node arrangement, oval shape, and serrated margin, ranging from 4 to 15 cm in length and 2 to 5 cm in width. Fragrant white blossoms, appearing either singly or in clusters, further enhance the tea plant's allure.

Tea, often consumed as a beverage second only to water, has been extensively researched for its medicinal properties. The beverage is crafted from the dried leaves of *C. sinensis*, which contain various polyphenols, notably flavanols, gallic acid, and catechins. These polyphenols constitute a significant portion of 30 to 40% of the extractable solids in dry green tea leaves. Among the primary catechins found in tea are epicatechin, epicatechin-3-gallate, epigallocatechin, and epigallocatechin-3-gallate (EGCG), known

for their high concentration. Widely utilised in traditional medicine systems such as Ayurveda, Unani, and Homoeopathy, the tea plant holds cultural and medicinal significance among tribal communities across India, China, and beyond. Consequently, extracting these tea polyphenols for medicinal purposes has garnered considerable attention in scientific research, underscoring the plant's therapeutic potential (Foster, 2002; Namita et al., 2012).

The detailed analysis of *Camellia sinensis* leaf microstructures across different stem nodes is particularly intriguing. Mature tea leaves often exhibit an increase in mechanical tissues as part of their defence mechanisms. This phenomenon underscores the dynamic interplay between plant anatomy and its adaptive strategies (Metcalfe et al., 1950; Das et al., 2012; Pamila et al., 2018). The article deals with a detailed study of the microstructures of *C. sinensis* leaves from different stem nodes.

Material and methods

Source of plant

The drought-resistant tea variety UPASI-9, developed through grafting from biclonal seed stocks, was generously provided by Hindustan Unilever Ltd., Bangalore. Ten saplings of this variety were transplanted into standard nutrient soil with a slightly acidic pH, as per requirements, and nurtured for six months in the greenhouse facilities at Ramniranjan Jhunjhunwala College, Ghatkopar, Mumbai, India.

Upon reaching a uniform height suitable for sampling, indicative of similar leaf age and size across saplings, a stratified random sampling approach was employed. From each of the ten plants, one leaf was carefully selected from the seven different nodal segments (Node 1 – young followed by older one), ensuring they were healthy and devoid of any infections or stressors.

Fixation of plant tissue

The leaves were gathered, cleaned, and trimmed to sizes ranging from 1 to 1.5 cm^2 before being immersed in a fixative solution composed of Formalin (5 mL), Acetic acid (5 mL), and 70% Ethyl alcohol (90 mL), known as FAA. Following a 24-hour fixation period, the specimens underwent dehydration using a graded series of tertiary-butyl alcohol, employing a well-established method outlined by Sass (1940) and Johansen (1940). Subsequently, the specimens were gradually infiltrated with paraffin wax (melting point 58-60°C) until the tertiary butyl alcohol solution reached supersaturation. This process facilitated the embedding of the specimens into paraffin blocks, following protocols described by Das et al. (2012) and Pamila et al. (2018).

Tea leaf sectioning

Microtomy work was done at the Plant Anatomy Research Centre in Chennai. Using a rotary microtome, the paraffin-embedded specimens were sectioned. Each section had a thickness ranging between 10 and 12 µm. Subsequently, the sections underwent dewaxing, following a traditional procedure outlined by Johansen (1940).

Staining of tissue

The sections were stained with Toluidine blue in accordance with the method by O'Brien et al. (1964). Toluidine blue is a type of polychromatic stain which resolves the component cell types by colouring in

various types (shades) as listed in Table 1. When necessary, sections were stained with safranin, fast green, and IKI (for starch identification). For the examination of stomatal morphology, venation patterns and trichome distribution, paradermal sections (taken parallel to the leaf surface) were utilized. Epidermal peeling was facilitated by leaf clearing using a 5% (w/v) sodium hydroxide solution, aided by partial maceration with Jeffrey's maceration fluid (Sass, 1940). Provisional preparations of the macerated/cleared materials were made using glycerine mounts. Additionally, powdered materials from various parts were cleared with NaOH, stained, and mounted in a glycerine medium to examine different cell components.

Photomicrographs

Table 1. Tissue colour observed after staining with Toluidine blue (adapted from O' Brein et al., 1964)

Tissue	Colour
Cellulose	Pink
Lignin	Blue
Suberin	Dark green
Mucilage	Violet
Protein	Blue
Collenchyma & parenchyma	Reddish purple
Callose & starch	Unstained

Microscopic examinations of tissues were complemented with relevant photomicrographs as needed. Images at various magnifications were captured using a Nikon Labophot 2 binocular microscope equipped with a CF optical system and a 6-volt, 20-watt Kohler illumination system comprising a halogen lamp and illuminator controller. Normal observations were conducted using a wide range of Nikon bright-field objectives. For the examination of crystals, starch grains, and lignified cells, polarized light microscopy was employed. These structures exhibit birefringent properties, causing them to appear bright against a dark background under polarized light. Scale-bars were included in the figures to indicate magnifications. The anatomical features were described in accordance with the terminology (Table 2) outlined by Esau (1964, 1977).

Table 2. Abbreviations used in figures (photomicrographs)

Abe: Abaxial epidermis	
LM: Leaf margin	
AC: Air chamber	
LV: Lateral view	
Ade: Adaxial epidermis	
MR: Midrib	
Adh: Adaxial hump	
Ph: Phloem	
Ads: Adaxial side	
PM: Palisade mesophyll	
Cu: Cuticle	
SC: Sclerenchyma	
Dr: Druses	
Scl: Sclereid	
DPP: Dilated phloem parenchyma	
SM: Spongy mesophyll	
EP: Epidermis	
St: Stomata	
GT: Ground tissue	
X: Xylem	
La: Lamina	
XF: Xylem fibres	

Results

Comparative analysis of leaf (entire) microstructures in Camellia sinensis across various stem nodes

Stem Node 01- The leaf features a noticeable midrib and robust lamina. The midrib, 440 µm thick, has a biconvex shape

with an elevated adaxial portion forming a wide hump (370 µm wide), while the abaxial part is semicircular and 570 µm thick. The vascular strand, 120 µm thick and 400 µm wide, consists of several vertical parallel lines of xylem elements. Phloem comprises wide parenchyma cells and small clusters of narrow, darkly stained sieve elements; (Fig. 1 A, B).

Stem Node 02- The leaf is bifacial with a prominently protruding midrib and heterofacial lamina. The midrib, 600 µm thick, has a short, wide abaxial hump and a thick, broad abaxial part. While the adaxial part measures 400 µm wide, the abaxial part is 700 µm wide. The vascular strand, 450 µm wide and 150 µm thick, features short to fairly long parallel lines of xylem elements with phloem elements distributed along the abaxial arc (Fig. 2 A, B, C).

Stem Node 03- The leaf exhibits a wide and thick adaxial hump and a broad semicircular abaxial midrib. The midrib, 850 µm thick, includes thick-walled cells in the adaxial epidermis and small, slightly papillate cells in the abaxial epidermis. The ground tissue comprises small parenchyma cells with a sparse distribution of brachysclereids. The vascular strand, 400 µm wide and 250 µm thick, consists of long, thin parallel lines of xylem elements, with phloem occurring in uniseriate small clusters; (Fig. 3 A, B, C).

Stem Node 04- The leaf features a robust midrib and a slender, smooth lamina. The midrib, 1.1 mm thick, has a short, wide adaxial hump and a broad, thick abaxial portion. The vascular strand, 450 µm thick and 1 mm wide, contains long, straight lines of xylem elements and a thick arc of phloem on the abaxial side; (Fig. 4 A, B, C)

Stem Node 05- The leaf exhibits a thick, smooth lamina and a biconvex midrib, 900 µm thick, with an adaxial hump (500 µm thick) and a wide abaxial part. The vascular strand, singular and extending horizontally for 850 µm, comprises compact parallel lines of xylem elements with thick phloem containing numerous sieve elements; (Fig. 5 A, B, C).

Stem Node 06- The vascular strand, 1 mm wide and 450 µm thick, is surrounded by sclerenchyma cells and comprises long, parallel lines of xylem elements with thick phloem on the abaxial side; (Fig. 6 A, B, C).

Stem Node 07- The leaf is bilaterally symmetrical with a prominent midrib and thick, smooth lamina. The midrib, 1 mm thick, features vertically oblong cells in the adaxial epidermis and small, papillate cells in the abaxial epidermis. The vascular strand, 1 mm thick, contains numerous xylem elements and a thin arc of phloem on the abaxial side: (Fig. 7 A, B, C).

Comparative analysis of leaf lamina microstructures in C. sinensis across various stem nodes

Stem Node 01- The leaf lamina is 180 µm thick, exhibiting heterofacial (bifacial) characteristics with distinct adaxial and abaxial sides. Adaxial epidermis comprises spindle-shaped or narrow rectangular cells with prominent cuticles, while the abaxial epidermis is apostomatic, featuring small squarish cells with thin walls. Palisade cells measure 40 µm in height (Fig. 1 C, D).

Stem Node 02- Lamina thickness measures 150 µm, with thin epidermal layers on both adaxial and abaxial sides comprising rectangular and squarish cells. Palisade layer consists of a single row of

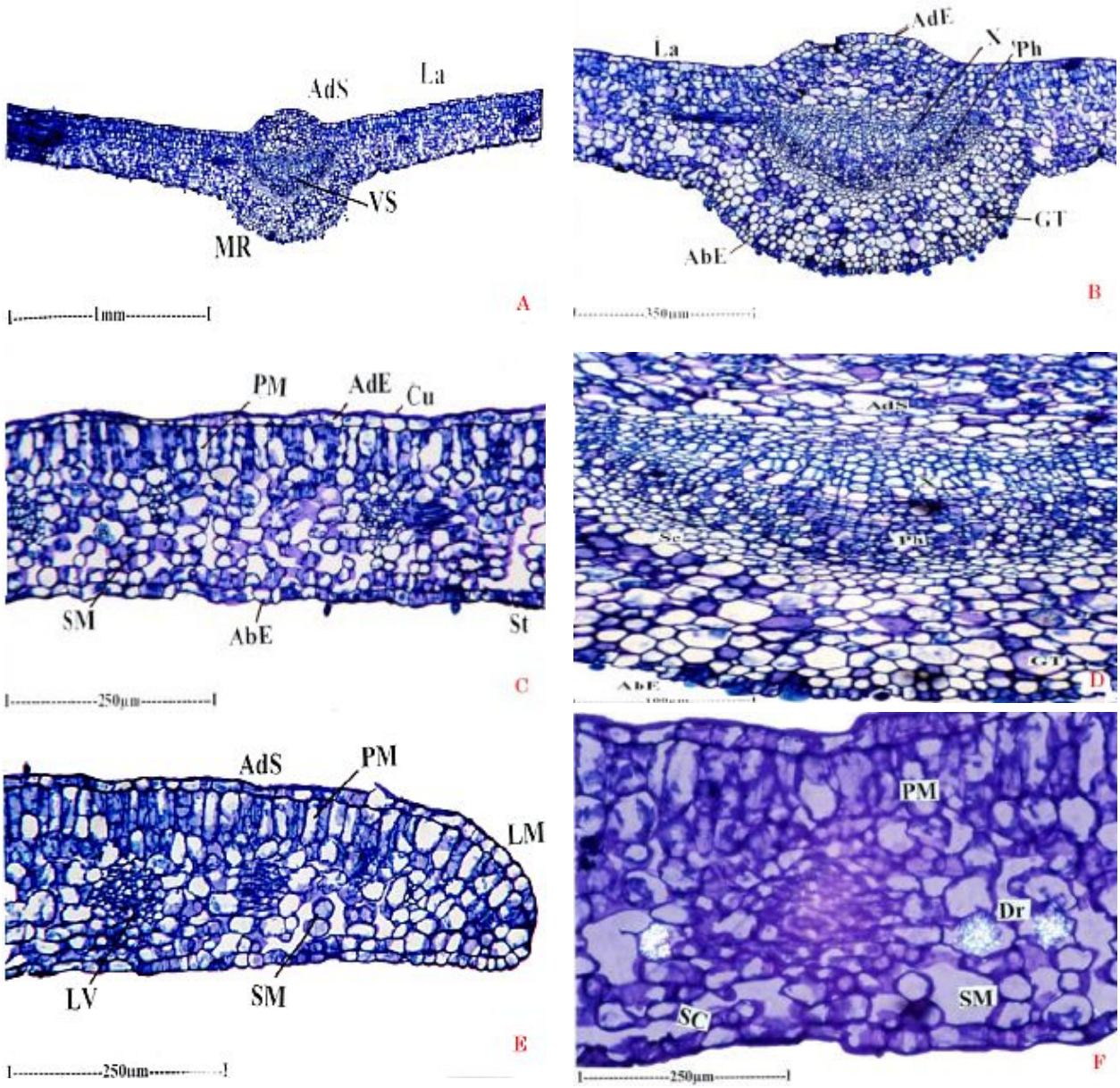

Fig. 1. A – Transverse section of node 1 leaf (4X), B – Transverse section of the midrib of node 1 leaf (10X), C – Transverse section of lamina of node 1 leaf (16X), D – Transverse section of the midrib (enlarged view) of node 1 leaf (40X), E – Transverse section of margin of node 1 leaf (16X), F – Transverse section of lamina showing druses (polarized light) of node1 leaf (16X)

short, cylindrical, compact cells measuring 30 µm in height. Spongy parenchyma exhibits smaller, less compact cells, approximately eight layered with the height of 60 µm (Fig. 2 D).

Stem Node 03- Lamina thickness is 250 µm, displaying bifacial symmetry with distinct adaxial and abaxial sides. Adaxial epidermis comprises vertically oblong, thick-walled cells, while abaxial epidermal cells are small, rounded, or squarish, and

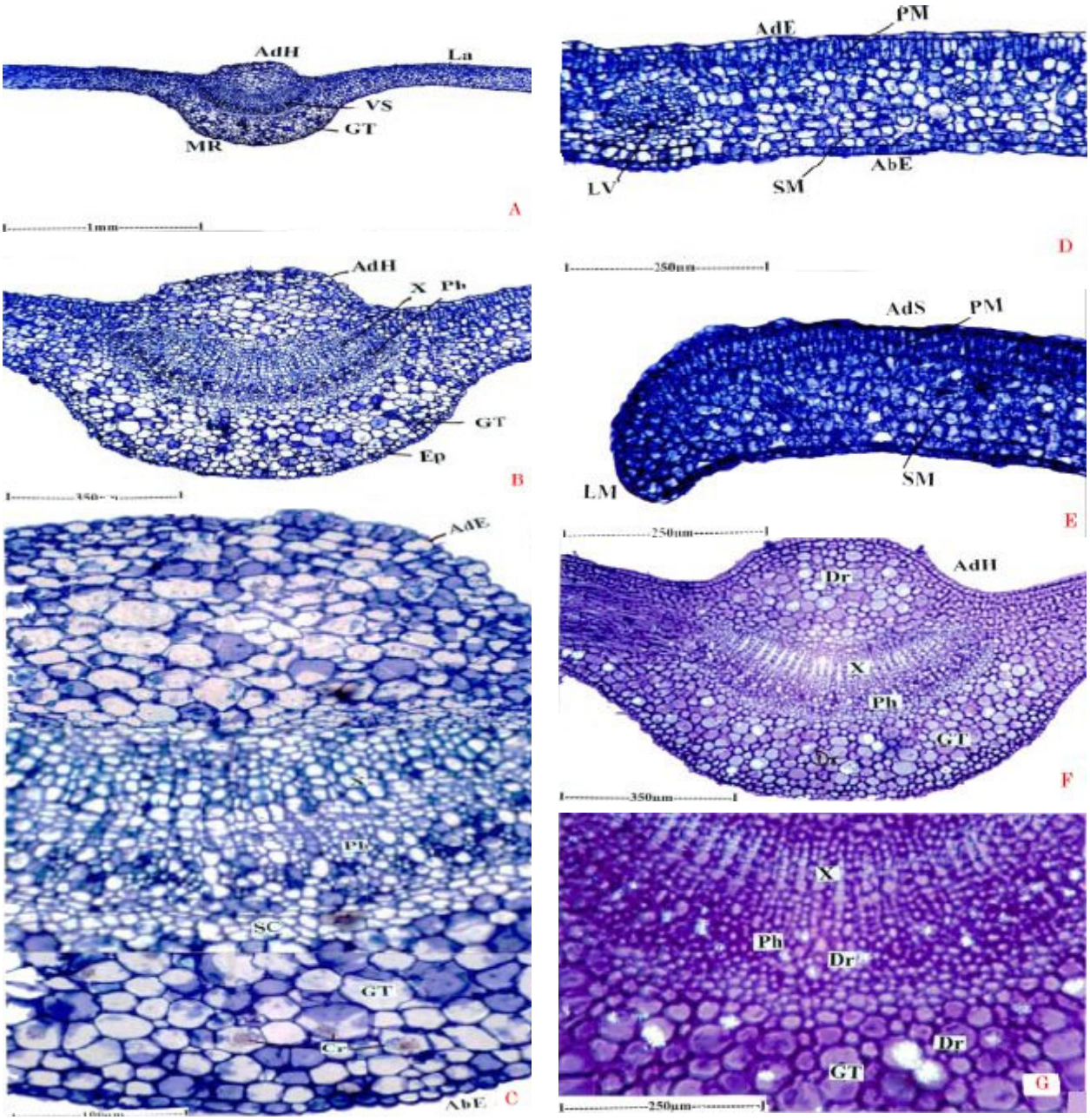

Fig. 2. A – Transverse section of node 2 leaf (4X), B – Transverse section of the midrib of node 2 leaf (10X), C – Transverse section of the midrib (enlarged view) of node 2 leaf (40X), D – Transverse section of lamina of node 2 leaf (16X), E – Transverse section of margin of node 2 leaf (16X), F – Transverse section of midrib showing the distribution of druses (polarized light) of node 2 leaf (10X), G – Transverse section of midrib showing the distribution of druses (enlarged) of node 2 leaf (16X)

thick-walled. Palisade band consists of two layers of cylindrical compact cells, 90 µm high, while the spongy parenchyma zone comprises about seven layers of spherical or lobed cells (Fig. 3 D).

Stem Node 04- Lamina thickness is 300 µm, and hypostomatic. Adaxial and abaxial epidermal cells are similar in shape and size, both being rectangular and thick-walled. Palisade cells measure 50 µm in height, forming a single layer of short,

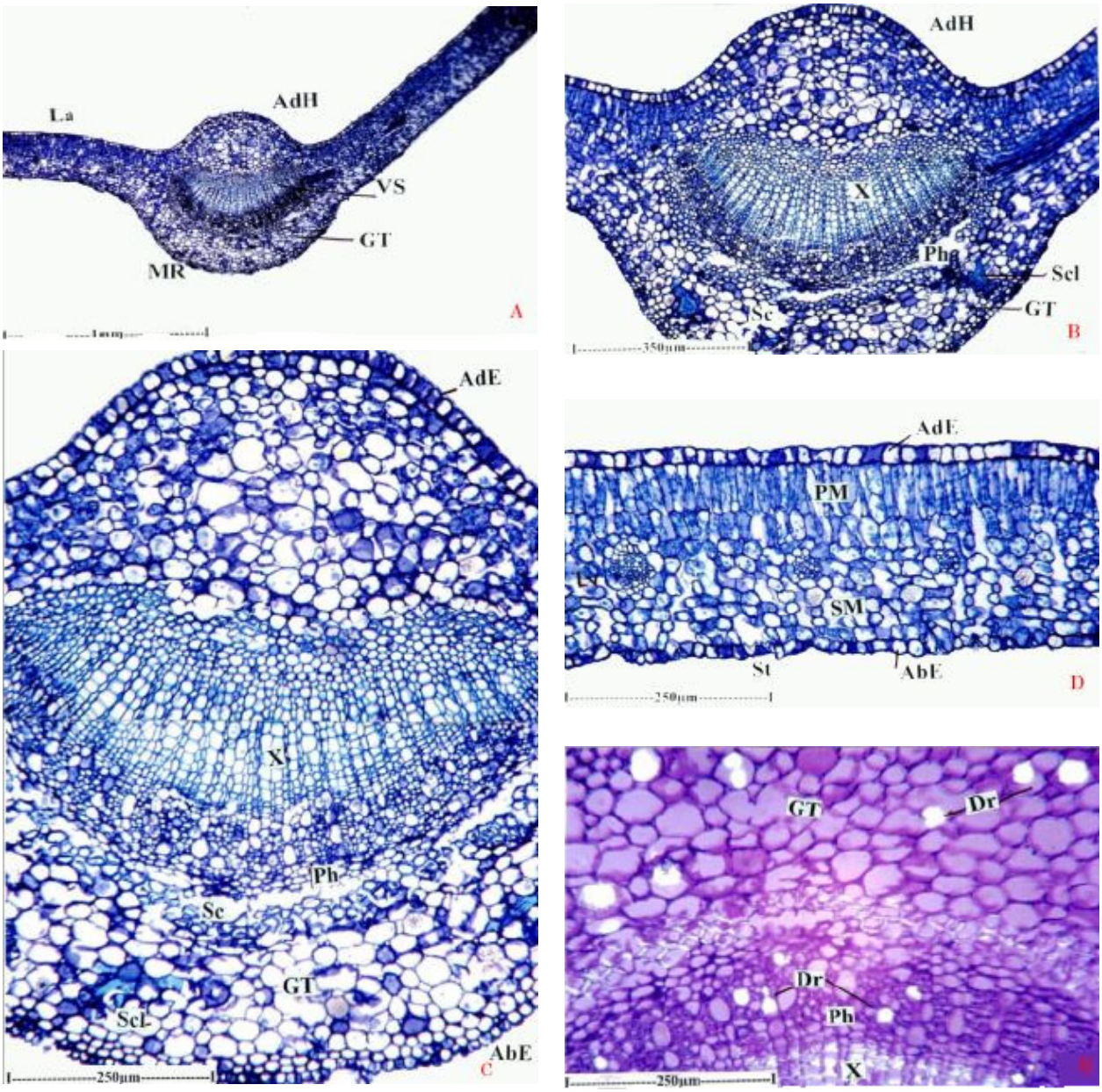

Fig. 3. A – Transverse section of node 3 leaf (4X), B – Transverse section of the midrib of node 3 leaf (10X), C – Transverse section of the midrib (enlarged view) of node 3 leaf (16X), D – Transverse section of lamina of node 3 leaf (16X), E –Transverse section of midrib showing the distribution of druses (polarized light) of node 3 leaf (16X)

cylindrical, less compact cells. Spongy parenchyma comprises 10-12 layered cells, small and spherical, forming a network of filaments enveloping wide air chambers (Fig. 4 D).

Stem Node 05- Lamina is 240 µm thick, smooth, and even on both surfaces. Adaxial epidermal cells are 20 µm thick and rectangular, while abaxial epidermal cells are spindle-shaped, thin-walled, and stomatiferous. Mesophyll tissues comprise two layers of cylindrical vertical palisade cells and about eight layers of loosely arranged spherical lobed spongy

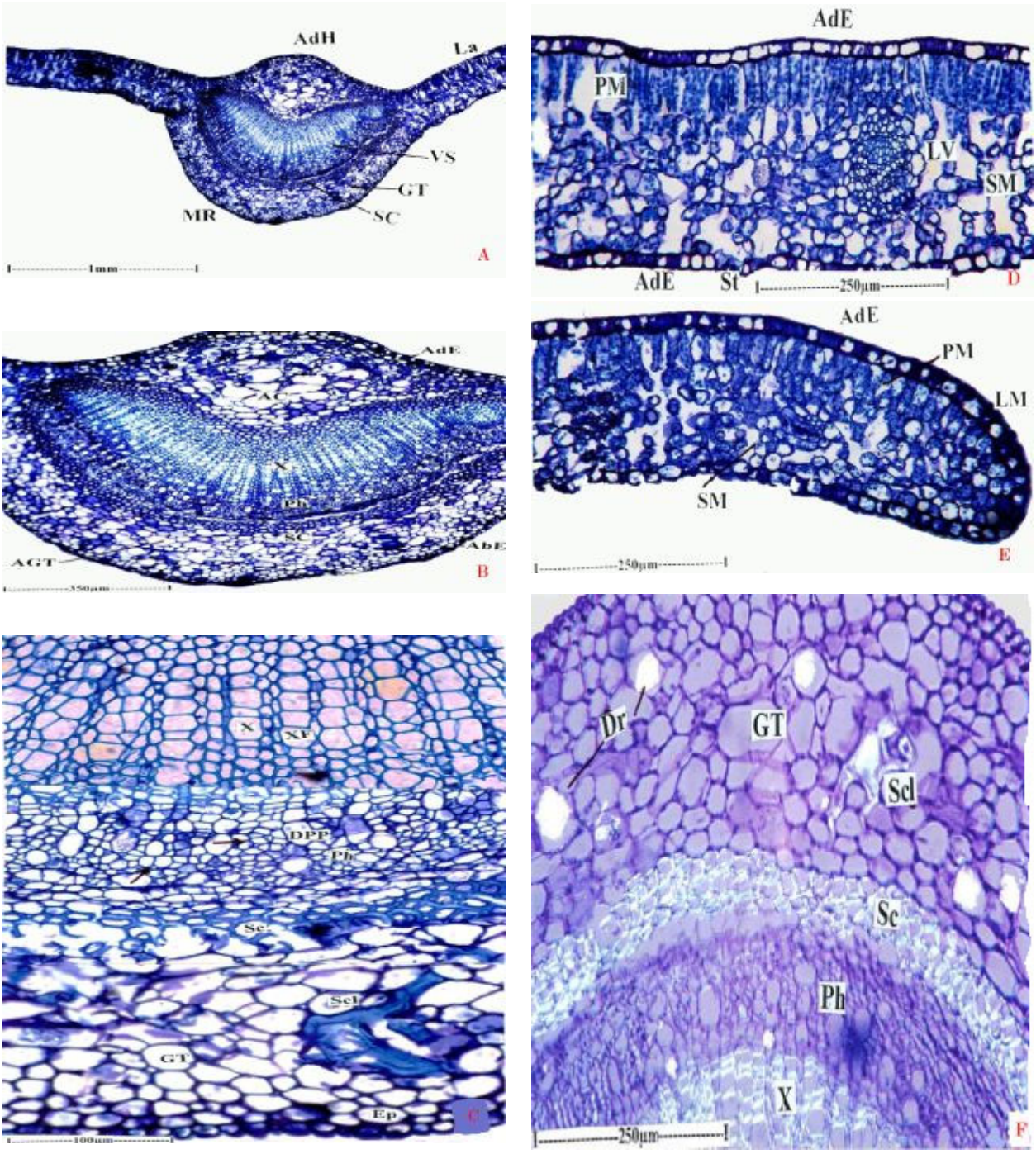

Fig. 4. A – Transverse section of node 4 leaf (4X), B – Transverse section of the midrib of node 4 leaf (10X), C – Transverse section of the midrib (enlarged view) of node 4 leaf (40X), D – Transverse section of lamina of node 4 leaf (16X), E – Transverse section of margin of node 4 leaf (16X), F – Transverse section of lamina showing druses (polarized light) of node 4 leaf (16X)

parenchyma cells, with vertically aligned sclereids (Fig. 5 D).

Stem Node 06- Lamina thickness is 290 µm, hypostomatic, with smooth and even surfaces. Both adaxial and abaxial epidermal layers comprise tabular cells with thick walls. Palisade zone is 100 µm in height, consisting of upper longer cells

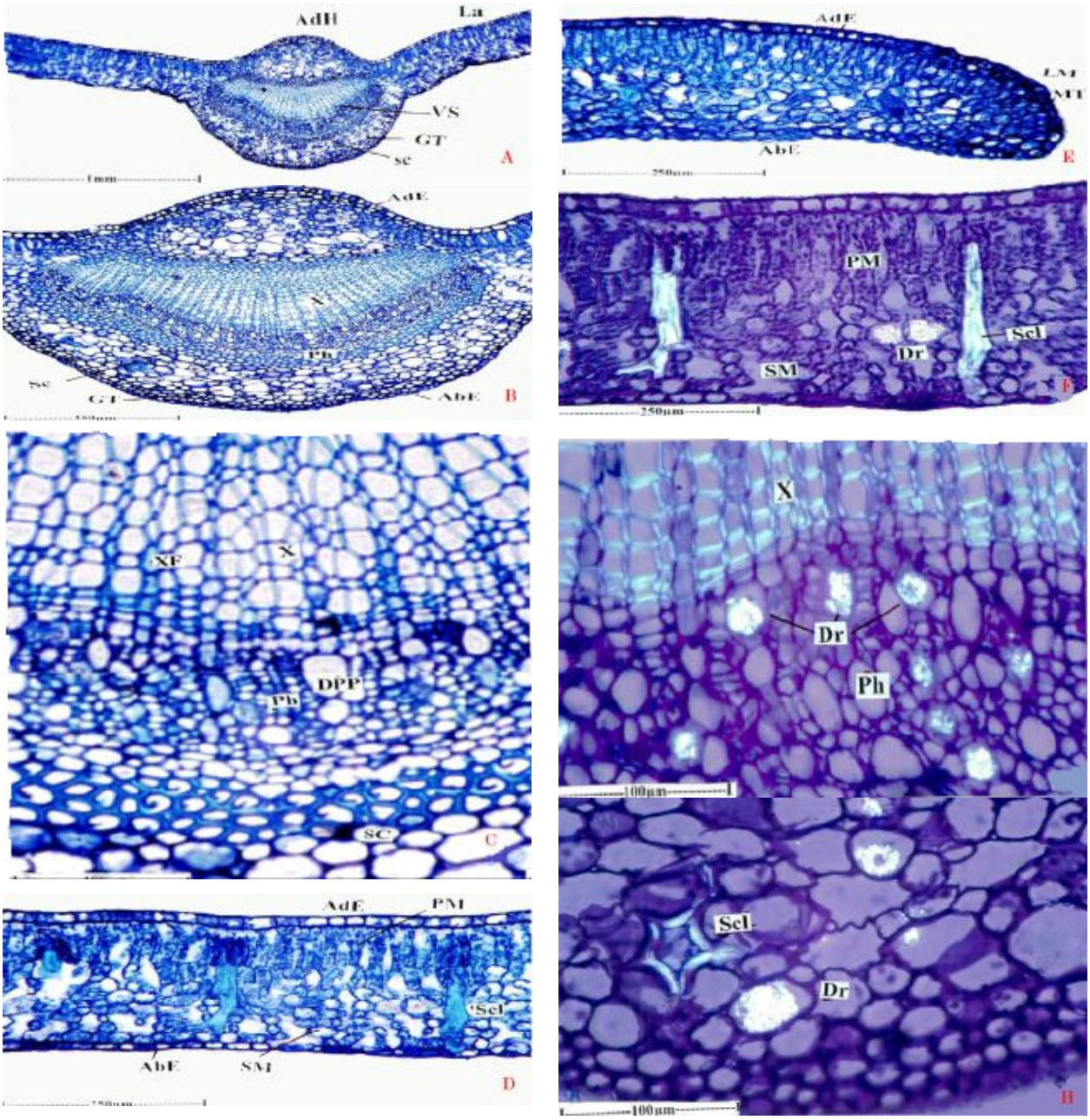

Fig. 5. A – Transverse section of node 5 leaf (4X), B – Transverse section of the midrib of node 5 leaf (10X), C – Transverse section of the midrib (enlarged view) of node 5 leaf (40X), D – Transverse section of lamina of node 5 leaf (16X), E – Transverse section of margin of node 5 leaf (16X), F – Transverse section of midrib showing the sclereids and druses (polarized light) of node 5 leaf (40X), G – Transverse section of midrib showing the sclereids, druses and styloids (polarized light) of node 5 leaf (40X)

and lower shorter cells. Spongy parenchyma comprises about eight layered cells, small, lobed (Fig. 6 D).

Stem Node 07- Lamina is distinctly dorsiventral, with adaxial and abaxial epidermal layers comprising tabular or squarish cells. Palisade zone is 130 µm in height, with cells arranged in two horizontal bands, narrowly cylindrical and less compact. Spongy parenchyma

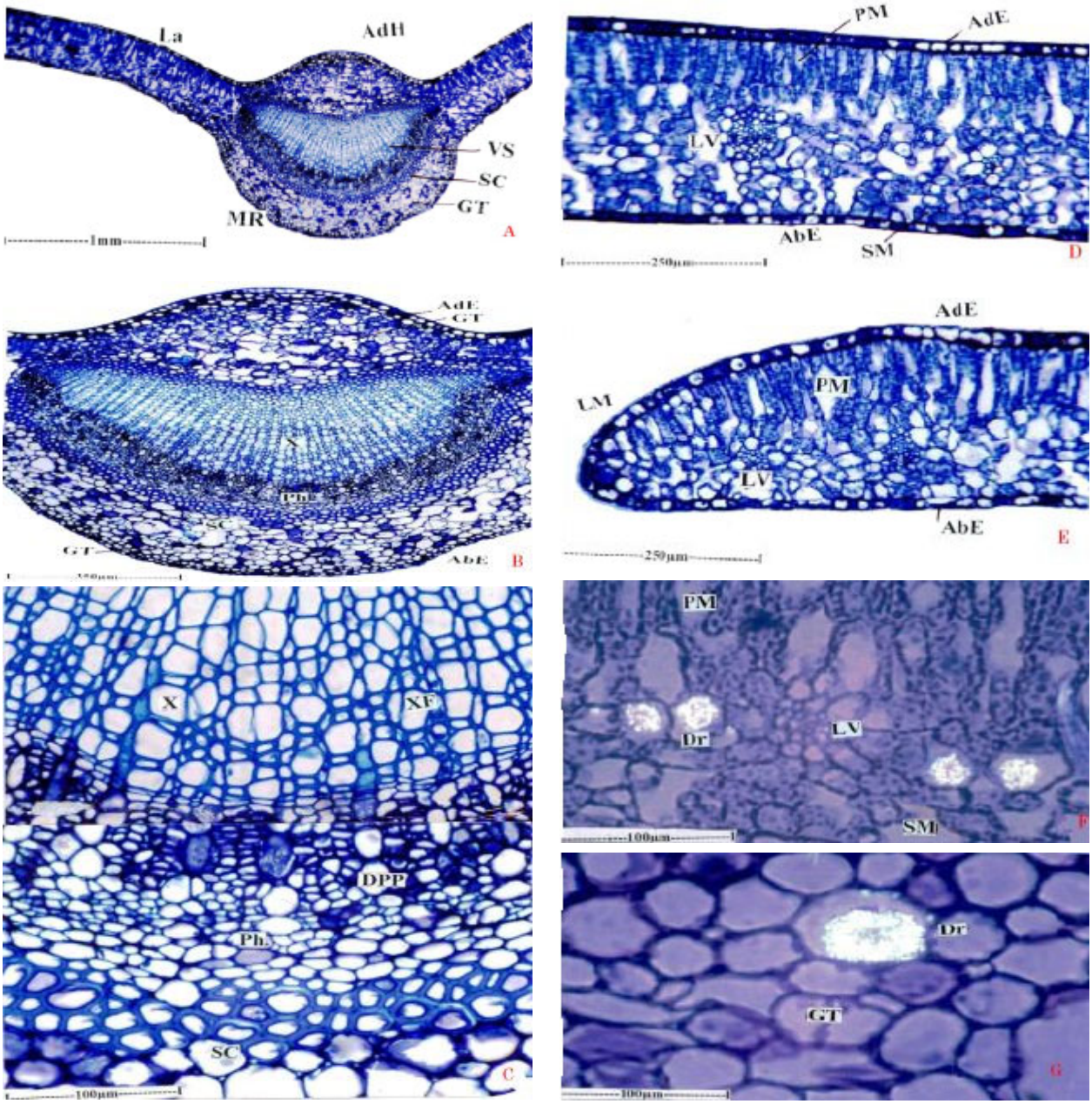

Fig. 6. A – Transverse section of node 6 leaf (4X), B – Transverse section of the midrib of node 6 leaf (10X), C – Transverse section of the midrib (enlarged view) of node 6 leaf (40X), D – Transverse section of lamina of node 6 leaf (16X), E – Transverse section of margin of node 6 leaf (16X), F – Druses in the mesophyll of node 6 leaf (40X), G – Druses in midrib-ground tissue of node 6 leaf (40X)

comprises about seven-layered cells, spherical and lobed, forming small air chambers. Vascular bundles are collateral and circular, with lateral veins located in the median part of the lamina (Fig. 7 D).

Comparative analysis of leaf margins microstructures in C. sinensis across various nodes

Stem Node 01- Marginal part thickness is 120 µm, bluntly conical with a semi-circular end. Adaxial epidermal cells are

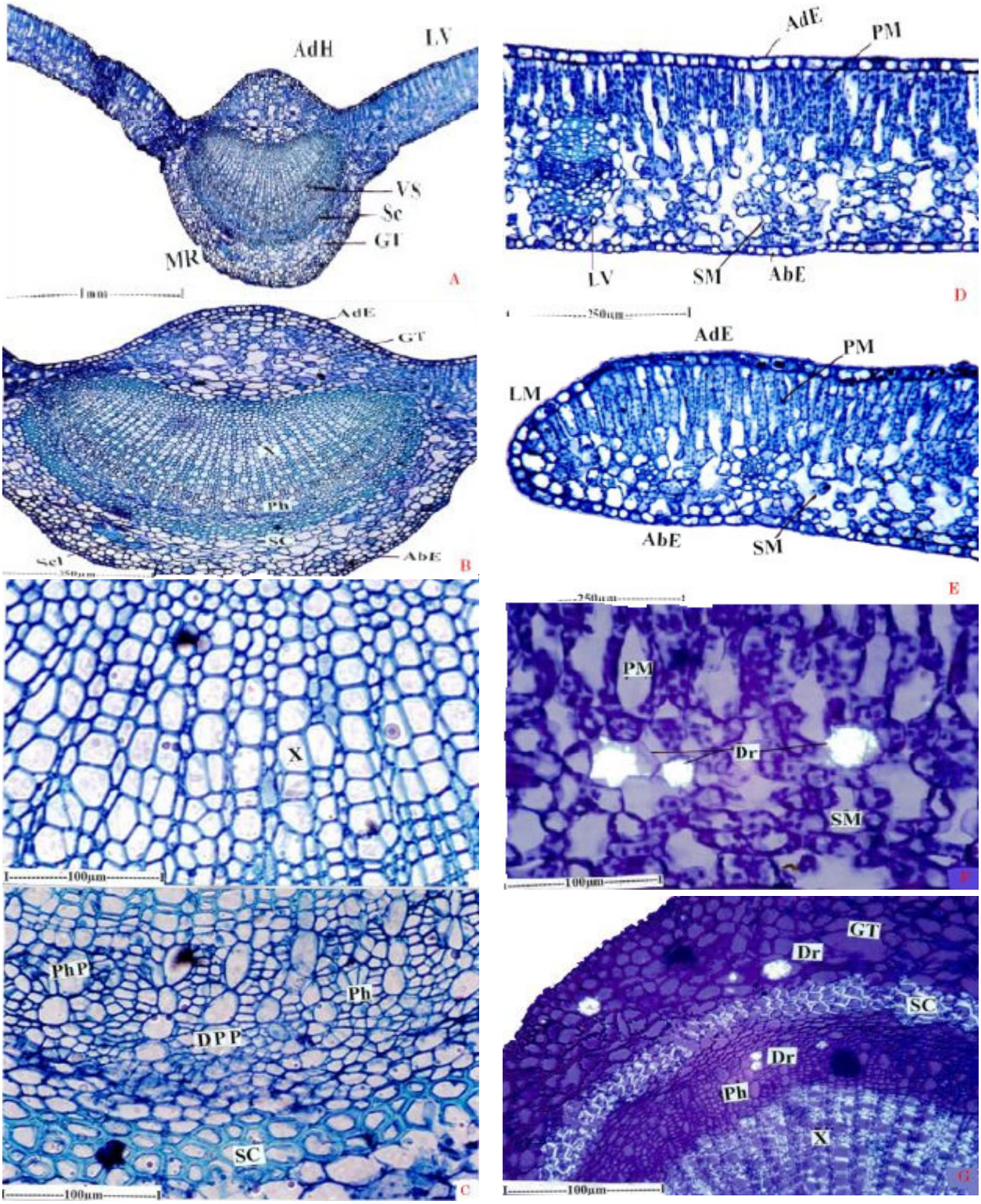

Fig. 7. A – Transverse section of node 7 leaf (4X), B – Transverse section of the midrib of node 7 leaf (10X), C – Transverse section of the midrib (enlarged view) of node 7 leaf (40X), D – Transverse section of lamina of node 7 leaf (16X), E – Transverse section of margin of node 7 leaf (16X), F – Druses in the mesophyll of node 7 leaf (40X), G – Transverse section of midrib, druses in the ground parenchyma and phloem parenchyma (as seen under polarized light) of node 7 leaf (40X)

horizontally elongated and tubular, while abaxial epidermal cells are small, squarish, and slightly thick-walled. Spongy mesophyll cells are small and compact with limited air spaces (Fig. 1 D, E).

Stem Node 02- Marginal part thickness measures 100 µm, blunt and conical, slightly bent down. Mesophyll tissues are not differentiated into palisade and spongy parenchyma cells, consisting of compact and homogeneous cells (Fig. 2 E).

Stem Node 03- Marginal part is thick, bluntly conical, and slightly bent down. Epidermal cells are thick with thick cuticles, and spongy mesophyll cells are compact with limited air spaces (Fig. 3).

Stem Node 04- Marginal end of the lamina is semicircular and 150 µm thick. Epidermal cells are very thick with thick cuticles, and undifferentiated mesophyll cells appear as compact, circular, thick-walled cells at the extreme margin (Fig. 4 E).

Stem Node 05- Marginal part thickness is 150 µm, slightly curved and semicircular. Epidermal cells along the semicircular part are small and thick-walled, with undifferentiated, compact and thick-walled mesophyll tissue (Fig. 5 E).

Stem Node 06- Marginal part thickness is 150 µm, conical with a semicircular end. Epidermal cells of the leaf margin are small and thick-walled. Palisade mesophyll cells are single-layered and short, retaining differentiation in the marginal part, while the spongy parenchyma is 3 or 4 layered with less compact cells (Fig. 6 E).

Stem Node 07- Leaf margin thickness measures 150 µm, slightly thin and conical. Epidermal cells become smaller and thick-walled along the marginal part, with retention of palisade-spongy mesophyll tissues in the marginal part (Fig. 7 E).

Comparative examination of crystal microstructures in C. sinensis leaves across different nodes

Stem Node 01- Calcium oxalate crystals of 60 µm in diameter druses are sparsely distributed within the unmodified ordinary cells with spongy parenchyma cells (Fig. 1 F).

Stem Node 02- Calcium oxalate druses are fairly abundant in the ground parenchyma of the midrib, less in the mesophyll tissue. They are diffuse in unmodified parenchyma cells. Small Druses are also located in the phloem zone (Fig. 2 F, G).

Stem Node 03- Calcium oxalate druses measuring 30 µm in diameter are common in the ground parenchyma cells and 20 µm wide in phloem parenchyma cells (Fig. 3 E).

Stem Node 04- The calcium oxalate druses are 40 µm wide sparsely distributed in the ground parenchyma of the midrib and also in the phloem parenchyma (Fig. 4 F).

Stem Node 05- Calcium oxalate druses are 30 µm in diameter, common in the leaf mesophyll in the phloem parenchyma cells, and ground parenchyma cells of the midrib. The crystals are sphaerocrystals i.e.,; druses with a central core of dark organic substance (Fig. 5 G, H).

Stem Node 06- Druses of calcium oxalate are 20-50 µm in diameter, sparse in the leaf mesophyll tissue. The druses also occur in ground parenchyma cells of the midrib (Fig. 6 F, G).

Stem Node 07- The calcium oxalate crystals druses are 10-15 µm in diameter, sparsely seen with palisade tissues and with ground parenchyma and phloem parenchyma of the midrib. The druses in the phloem zone are smaller than those in the outer ground tissue (Fig. 7 F, G). A summary of comparative analysis is listed in Table 3.

Table 3. Comparative analysis of anatomical features in tea leaves

Node	Observed area	Size (in µm)	Calcium oxalate crystals
1	Midrib, adaxial and abaxial hump	440,370 & 570	Sparse & druses are 60 µm in diameter
	Lamina	180	
	Leaf margin	120	
2	Midrib, adaxial and abaxial hump	600,400 & 700	Fairly abundant & druses are smaller in size
	Lamina	150	
	Leaf margin	100	
3	Midrib, adaxial and abaxial hump	850,550 & 800	Druses in the ground parenchyma cells are 30 µm & in phloem parenchyma cells are 20 µm wide
	Lamina	250	
	Leaf margin	120	
4	Adaxial hump	450	Sparse & druses are 40 µm wide
	Lamina	300	
	Leaf margin	150	
5	Midrib, adaxial and abaxial hump	900,500 & 900	Druses are 30 µm in diameter
	Lamina	240	
	Leaf margin	150	
6	Adaxial hump	550	Druses are 20-50 µm in diameter
	Lamina	290	
	Leaf margin	150	
7	Adaxial and abaxial hump	500 & 950	Druses are 10-15 µm in diameter
	Lamina	130	
	Leaf margin	150	

Discussion

Erxu et al. (2008) showed the diverse microstructures found within *Camellia sinensis* leaves, thus, offering valuable insights into systematic classification. Through the application of safranin and fast-green staining techniques, researchers observed a wide range of thicknesses in palisade and spongy tissues Johansen (1940). The correlation between leaf micromorphology and boron deficiency conditions, as highlighted by Hajiboland et al. (2012), provides intriguing insights into the impact of altered physical properties, such as extensibility and plasticity of cell walls, on cellular elongation. This correlation not only enhances our understanding of cell wall formation but also underscores the distinctiveness of micromorphological features influenced by environmental factors.

Study by Naing et al. (2019) reveals fascinating variations in leaf morphology and anatomy of *C. sinensis* plants from different localities. Variations in leaf and cell sizes, including the number and thickness of cell layers, were observed between different geographical regions, highlighting the dynamic nature of plant morphology in response to environmental factors. Our anatomical examination unveiled a bilateral leaf structure with a prominent midrib and a fairly thick smooth lamina. Notably, the midrib displayed variations in thickness and morphology, with distinct epidermal

characteristics observed on the adaxial and abaxial sides. Additionally, the intricate arrangement of ground tissue, vascular strands, and sclerenchyma sheaths further enriched the understanding of leaf anatomy and microstructural adaptations.

The present study investigated different regions of the leaf, including the lamina, leaf margins, and even the presence of calcium oxalate crystals. These analyses revealed the heterofacial nature of the lamina, the structural composition of leaf margins, and the distribution patterns of calcium oxalate crystals, each contributing to the intricate tapestry of tea leaf micromorphology. Intriguingly, the presence of sphaerocrystals, characterized by a central core of dark organic substance, within different tissue zones further underscores the complexity of tea leaf microstructures and their potential implications for physiological processes.

Tea quality hinges on cultivar, plucking standard, processing, storage, taste, aroma, and health benefits. Environmental factors like soil, climate, and altitude shape the flavour and aroma. Each cultivar offers distinct traits, with younger leaves boasting delicate flavours. Processing techniques, spanning withering to drying, determine tea types. Proper storage ensures freshness. Taste and aroma, subjective and influenced by preferences, enhance the sensory experience. Health benefits, including antioxidants and vitamins, contribute to value. Assessing quality requires a holistic view, considering personal preferences and cultural traditions. Standardising these factors for specific products can be aided by microstructure data analysis in tea production.

Conclusion

The revelation that older leaves of the *C. sinensis* plant exhibit well-developed and diverse microstructures compared to younger leaves opens up a plethora of fascinating applications in the studied variety. Firstly, these detailed studies of microstructures play a crucial role in species validation and identification. By analysing the unique patterns and arrangements of stomata, leaf venation, and other microstructural features, we can accurately distinguish between different tea varieties and even detect potential adulteration or mislabelling in tea products. This is particularly important in ensuring product authenticity and maintaining quality standards in the tea industry.

In summary, the detailed study of microstructures in *C. sinensis* leaves holds immense promise for a wide range of applications, from ensuring product authenticity and quality to optimizing tea processing techniques and advancing agricultural practices. By leveraging this knowledge, other researchers and industry professionals can unlock new opportunities for innovation and improvement in the fascinating world of tea.

Acknowledgements

The authors express gratitude to Dr. P. Jayaraman, Director of the Plant Anatomy Research Centre (Chennai), for his invaluable assistance with anatomical studies. Additionally, the authors extend their appreciation to HUL (Hindustan Unilever) for providing financial support for the collaborative research project.

References

Das C, Dash SK & Sahoo DC 2012. Macroscopical and microscopical study of *Tecoma stans* Linn. leaf. Research Journal of Pharmaceutical, Biological and Chemical Sciences, 3(2): 100-107.

Erxu PI, Qiufa P, Hongfei L, Jingbo S, Yueqiang D, Feilai H & Hui H 2009. Leaf morphology and anatomy of *Camellia* section Camellia (Theaceae). Botanical Journal of the Linnean Society, 159(3): 456-476.

Esau K 1977. Anatomy of Seed Plants. John Wiley & Sons. Inc. New York.

Esau K 1964. Plant Anatomy. John Wiley & Sons. Inc, New York, London, Sydney, 167 pages.

Foster S 2002. *Camellia sinensis* (Green tea). Alternative Medicine Review Monographs, 2002: 200-204.

Hajiboland R, Farhanghi F & Aliasgharpour M 2012. Morphological and anatomical modifications in leaf, stem and roots of four plant species under boron deficiency conditions. Anales de Biología, 34: 15-29.

Johansen DA 1940. Plant Microtechnique. McGraw Hill Book Co., New York.

Metcalfe CR & Chalk L 1950. Anatomy of the Dicotyledons, volume I. Clarendon Press, Oxford.

Naing YY, Khaing WW & Kywe T 2019. Morphological and Anatomical Characteristics of *Camellia sinensis* (L.) Kuntze from Two Different Localities. Doctoral dissertation, MERAL Portal.

Namita P, Mukesh R & Vijay KJ 2012. *Camellia sinensis* (Green Tea): A Review. Global Journal of Pharmacology, 6(2): 52-59.

O'Brien T, Feder N & McCully ME 1964. Polychromatic staining of plant cell walls by toluidine blue O. Protoplasma, 59(2): 368-373.

Pamila A, Karpagam S & Jayaraman P 2018. Morphological and anatomical features of *Alternanthera bettzickiana* (regel) g. Nicholson. International Journal of Botany and Research, 8(6): 5-18.

Sass JE 1940. Elements of Botanical Microtechnique. McGraw Hill Book Co., New York.